

# polymer review

## The interpretation of orientation–strain relationships in rubbers and thermoplastics

G. R. Mitchell,\* D. J. Brown and A. H. Windle

University of Cambridge, Department of Metallurgy and Materials Science,

Pembroke Street, Cambridge CB2 3QZ, UK

(Received 30 January 1985)

The orientation–strain behaviour typical of non-crystalline polymers is examined with reference to new techniques for determining molecular orientation parameters in a variety of crosslinked and thermoplastic materials, as well as the long-established methods based on the optical anisotropy of natural rubber. It is shown that the affinely-deforming ‘random chain’ assumed by conventional theory is not successful in predicting the relationship between chain orientation and strain unless the network is assumed to change significantly with strain. The implications of this observation are discussed in terms of the behaviour of crosslinks and entanglements: the conventional view of anisotropy needs to be supplemented by an approach in which orientation and strain are seen as distinct aspects of a polymer’s response to the stress imposed upon it.

(Keywords: orientation; entanglements; natural rubber; poly(methyl methacrylate); poly(ethylene terephthalate); poly(vinyl chloride))

### MOLECULAR ORIENTATION IN RUBBER-LIKE POLYMERS

Our understanding of the development of molecular orientation in non-crystalline polymers owes much to early advances in the theory of rubber-like elasticity, commencing with the work of Kuhn and Gr $\ddot{u}$ n<sup>1–3</sup> and engagingly described by Treloar<sup>4</sup>. This statistical theory of entropy-driven elasticity and consequent optical anisotropy was based upon the concept of a random chain of  $n$  links undergoing affine deformation (i.e. as if the chain ends were embedded in an elastic continuum). The polymeric system is taken to comprise a network of such chains, joined by permanent chemical crosslinks, with overall properties obtainable by simply summing the contributions of the individual chains. This is equivalent to saying that *intermolecular* interactions are of negligible consequence in comparison to *intramolecular* effects. The slightly later approaches involving a network of ‘phantom chains’<sup>5,6</sup> start from somewhat different assumptions but lead to similar results: the equations for stress–strain behaviour differ only by a small numerical factor, and the prediction is made that the mean positions of chain junctions will indeed change affinely with strain.

This view of rubbery elasticity and anisotropy largely took shape in a period when the ranges both of known polymers and of available techniques were restricted. It was thus inevitable that early comparisons between theory and experiment centred upon the optical anisotropy or *birefringence* ( $\Delta\mu$ ) of natural rubber (*cis*-polyisoprene)<sup>7–11</sup> and of closely-related materials such as gutta-percha (*trans*-polyisoprene)<sup>9,10</sup> and polyethylene<sup>10,12</sup>. In more recent years a variety of spectroscopic techniques has become available, encompassing infra-red dichroism, laser-Raman spectroscopy, nuclear magnetic resonance (n.m.r.) spectroscopy, polarized

fluorescence, and wide-angle X-ray scattering (WAXS). The essential features of each technique have been reviewed elsewhere<sup>13–15</sup>.

The value of these newer techniques may be appreciated by considering the orientation distribution function  $\rho(\phi)$  for molecular units aligned about a unique axis (we take uniaxial symmetry for simplicity). Here,  $\rho(\phi)d\phi$  represents the fraction of units whose individual axes or ‘directors’ lie at angles in the range  $\phi$  to  $\phi+d\phi$  to the unique axis, typically a fibre draw direction.  $\rho(\phi)$  may be expressed as an infinite series of terms in powers of  $\cos\phi$ :

$$\rho(\phi) = \sum_{n=0}^{\infty} (n + \frac{1}{2}) \langle P_n(\cos\phi) \rangle P_n(\cos\phi)$$

where the coefficients  $P_n$  are Legendre polynomials. The angle brackets denote mean values, so that  $\langle P_n(\cos\phi) \rangle$  represents the amplitude of the function  $P_n$ . Only the terms in the series with even  $n$  are non-zero. Such an expression amounts to the analysis of the function  $\rho(\phi)$  into spherical harmonics, much as the waveform can be analysed into Fourier components.

The newer techniques for orientation determination afford an advance over optical birefringence in three significant respects. Firstly, birefringence is simply proportional to  $\langle P_2 \rangle$ : it thus yields only the first term in the series, albeit the most important one. Other methods in principle allow several terms to be determined. Secondly, birefringence measurements under load are complicated by the possibility that part of the measured anisotropy corresponds to stress birefringence (i.e. due to the distortion of intermolecular and intramolecular spacings, or the rotation of pendant groups, by the applied stress) rather than resulting from chain orientation. Newer techniques avoid this difficulty. Thirdly, such techniques provide *absolute* values of  $\langle P_n \rangle$ , while birefringence affords only a *relative* measure of  $\langle P_2 \rangle$ . If the maximum possible orientational birefringence can be calculated—the so-

\* Present address: J. J. Thomson Laboratory, University of Reading, Whiteknights, Reading RG6 2AF, UK.

called *intrinsic* birefringence,  $\Delta\mu_0$ , corresponding to the hypothetical situation where all orienting units in the system are perfectly aligned with the unique axis—then the utility of birefringence data is greatly enhanced. By correlating spectroscopic and optical measurements, a value for  $\Delta\mu_0$  can indeed be deduced.

The availability of a range of synthetic thermoplastics has also afforded an advance in the understanding of orientation. Many have glass transitions somewhat above room temperature, allowing measurements to be made after quenching from the rubbery regime (which for a thermoplastic implies, of course, rubberlike within the experimental timescale) to room temperature and unloading, avoiding complications due to stress birefringence and allowing easy comparison with measurements on specimens deformed in the glassy state.

Arguably the most powerful of the newer techniques is that of WAXS<sup>16,17</sup>. In principle it allows values of any of the  $\langle P_n \rangle$  to be obtained (though in practice terms beyond  $\langle P_4 \rangle$  are usually smaller in magnitude than the range of error in their determination). Furthermore, the method does not require that a particular conformational model be assumed first: it is possible within the same experiment both to determine the probable molecular conformation (including any propensity to change in conformation with strain) and to monitor the development of orientation. The method is discussed in detail elsewhere<sup>18,19</sup>: in particular, it has been employed to build up a detailed understanding of the structure and orientational behaviour of poly(methyl methacrylate) (PMMA).

Figure 1 shows data for the development of orientation in natural rubber. The birefringence data show the well-known upward curvature predicted by conventional rubber elasticity theory<sup>4,7</sup>. However, the absence of such a pronounced trend in the WAXS data (which refer only to the non-crystalline component of the material), and the fact that only the 20°C WAXS data show any noticeable

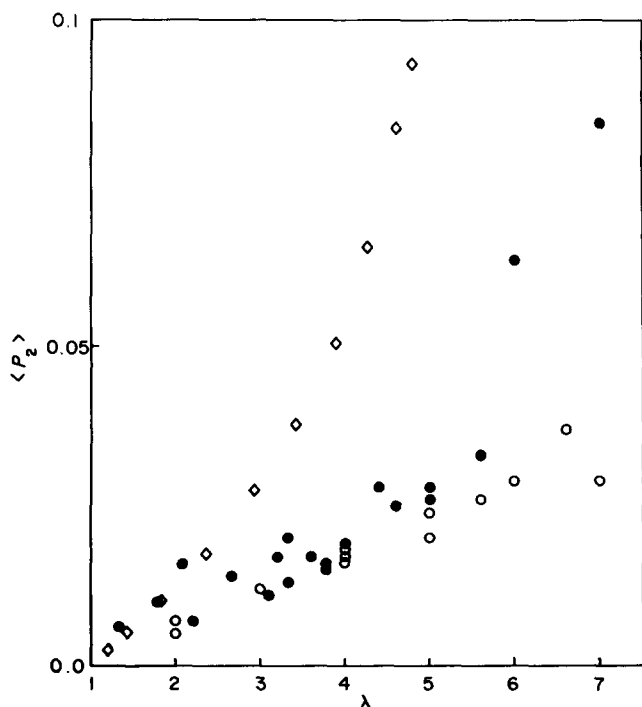


Figure 1 Orientation parameter  $\langle P_2 \rangle$  vs. extension ratio  $\lambda$  for cis-polyisoprene (natural rubber). Data: ( $\diamond$ ) birefringence, 25°C<sup>8</sup> assuming  $\Delta\mu_0 = 0.20^{20}$ ; ( $\bullet$ ) WAXS, 20°C<sup>20</sup>; ( $\circ$ ) WAXS 56°C<sup>20</sup>

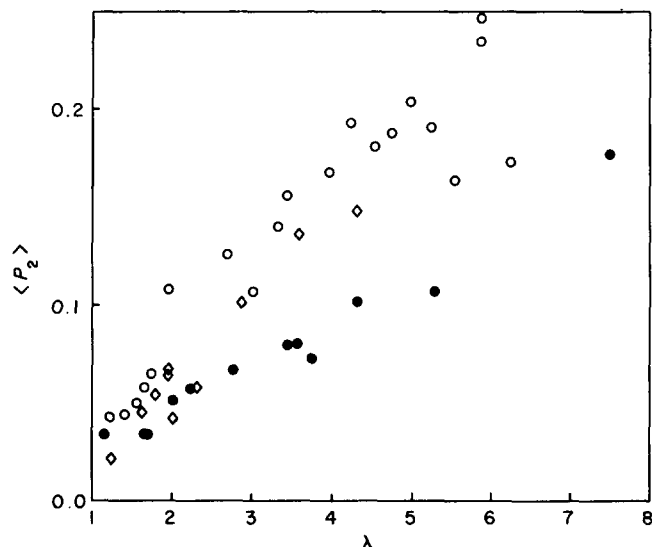


Figure 2 Orientation parameter  $\langle P_2 \rangle$  vs. extension ratio  $\lambda$  for PMMA above its glass transition. Data from wide-angle X-ray scattering (WAXS): ( $\circ$ ) plane strain compression, 125°C<sup>16,21</sup>; ( $\bullet$ ) plane strain compression, 150°C<sup>16,21</sup>; ( $\diamond$ ) uniaxial tension, 150°C<sup>22</sup>

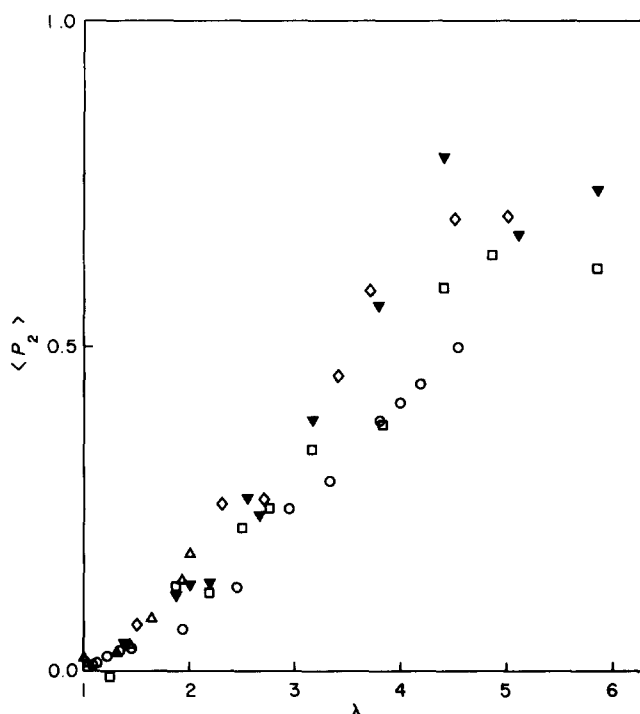


Figure 3 Orientation parameter  $\langle P_2 \rangle$  vs. extension ratio  $\lambda$  for PET drawn at 80°C: data from several techniques: ( $\circ$ ) birefringence<sup>23</sup>; ( $\diamond$ ) birefringence<sup>24</sup>; ( $\nabla$ ) polarized fluorescence<sup>25</sup>; ( $\triangle$ ) polarized fluorescence<sup>26</sup>; ( $\square$ ) laser-Raman spectroscopy, 1616 cm<sup>-1</sup> line (ref. 27, 'conformational model B')

curvature at all, lend weight to the possibility that the curvature is largely associated with strain-induced crystallization. This phenomenon will be particularly evident at lower temperatures and will add significantly to the  $\langle P_2 \rangle$  measured by optical methods.

In PMMA, a polymer showing no evidence of crystallization, such an upward curvature is absent (Figure 2): indeed, the data show if anything a downward curvature, the slope decreasing at higher strains. The overall slope is considerably greater than for natural rubber, however. Data for poly(ethylene terephthalate) (PET) drawn slightly above its glass transition show a still greater slope: Figure 3 depicts data obtained by several methods and

showing excellent agreement between the different techniques. Orientation-strain studies of PVC indicate a still steeper  $\langle P_2 \rangle$  vs. strain plot, but although it is claimed that the material used is of zero or very low crystallinity<sup>28</sup>, a question remains as to the extent to which this behaviour is a reflection of microcrystallite orientation. This possibility is underlined by the minor nature of any changes seen on passing through the glass transition (about 81°C). Figure 4 depicts data for a range of temperatures above and below  $T_g$ .

In predicting the orientation behaviour of a material displaying rubberlike elasticity, the affine model is quite unambiguous in indicating that the gradient of the  $\langle P_2 \rangle$ -strain plot will steadily increase from a low value at zero strain (in the elementary Kuhn-Grün model,  $0.6/n$  where  $n$  is the number of links in the equivalent random chain), and that this curvature will be more rapid for smaller values of  $n$ . It is clear from the data shown above that while this prediction may be valid for natural rubber at room temperature (though perhaps less so than a consideration of birefringence data alone would suggest), it is inapplicable to some important thermoplastics.

#### ORIENTATION BELOW THE GLASS TRANSITION

A comprehensive view of deformation behaviour must naturally encompass both rubbery and glassy regimes. It is not usual to try to interpret glassy deformation in terms of an affine network—the development of orientation with strain is far too rapid for such an attempt to succeed, quite apart from the radically different stress-strain behaviour—but a related treatment has been considered. This is the *pseudoaffine* deformation scheme, originally proposed by Kratky<sup>31</sup> and developed in detail by Ward and co-workers<sup>32</sup>.

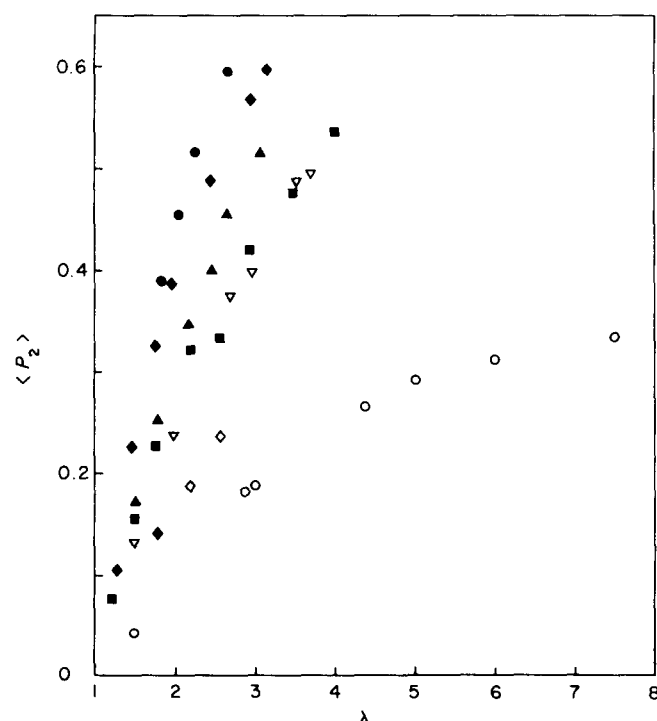


Figure 4 Orientation parameter  $\langle P_2 \rangle$  vs. extension ratio  $\lambda$  for PVC. Data from birefringence: (○) 90°C<sup>29</sup>; (◇) 80°C<sup>30</sup>; (▽) 90°C<sup>30</sup>; (●) 65°C<sup>28</sup>; (◆) 80°C<sup>28</sup>; (▲) 95°C<sup>28</sup>; (■) 110°C<sup>28</sup>; (▽) 125°C<sup>28</sup>

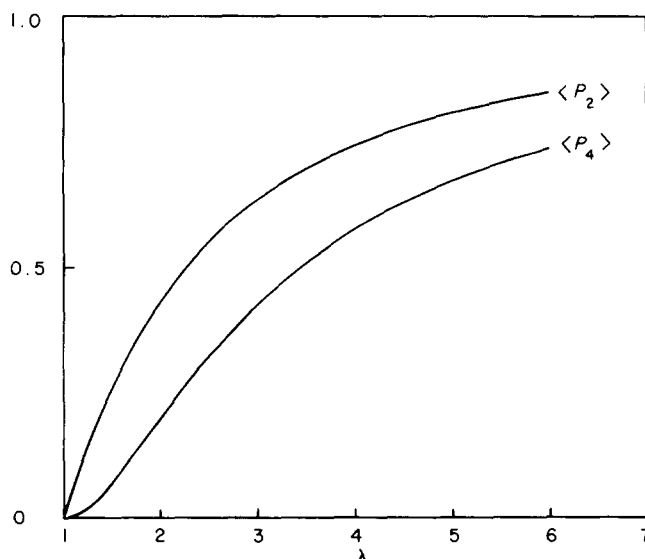


Figure 5  $\langle P_2 \rangle$  and  $\langle P_4 \rangle$  as functions of extension ratio  $\lambda$  according to the pseudoaffine deformation scheme

The pseudoaffine scheme describes the relationship between orientation and strain of rods of fixed length within an affinely deforming matrix (Figure 5), rather like needles in an affinely deforming haystack. Its primary application has been to the development of crystallite orientation, which it describes very satisfactorily; but the scheme has also been applied to orientation in polymer glasses, despite the obvious uncertainty as to the nature of the 'rods' in the glassy state. The pseudoaffine scheme describes the shape of the  $\langle P_2 \rangle$ -strain curve for a typical glassy polymer quite well (so it tends to fit birefringence-strain plots), but when absolute values of  $\langle P_2 \rangle$  are available, e.g. for PET<sup>33</sup> and PMMA<sup>22</sup>, it becomes clear that for a given strain the pseudoaffine model tends to predict too high a  $\langle P_2 \rangle$ . It is not possible to adjust the scaling, since the model contains no adjustable parameters. When higher order terms than  $\langle P_2 \rangle$  are taken into account, the pseudoaffine model again appears less than satisfactory: it predicts values of  $\langle P_4 \rangle$  very much in excess of those determined by WAXS or n.m.r. spectroscopy (though laser-Raman spectroscopy does predict rather higher values, closer to those of the pseudoaffine model).

On a more fundamental level, the pseudoaffine model retains the foundation assumption of its affine counterpart that orientation can be regarded as a function of strain alone. This assumption is wrong, as annealing and recovery studies demonstrate<sup>34</sup>. Finally, it is perhaps conceptually unsatisfactory that an approach to the glassy regime neglects the network nature of the system. Even below the glass transition a polymer remains an assemblage of entangled and perhaps crosslinked chains, and the importance of such a network picture has been clearly demonstrated by work on crazing in polymer glasses<sup>35</sup>.

Typical  $\langle P_2 \rangle$ -strain plots for non-crystalline polymers below  $T_g$  are shown in Figures 6 (for PMMA) and 7 (for PET). Plots relating to PVC are included in Figure 4, though the proviso above about possible microcrystallite orientation should again be noted. Figures 6 and 7 clearly show both the much higher chain orientation, as measured by  $\langle P_2 \rangle$ , associated with a given strain in a glass as compared to a rubber (cf. Figures 2 and 3), and the slight nature of any changes with temperature. However, Figure

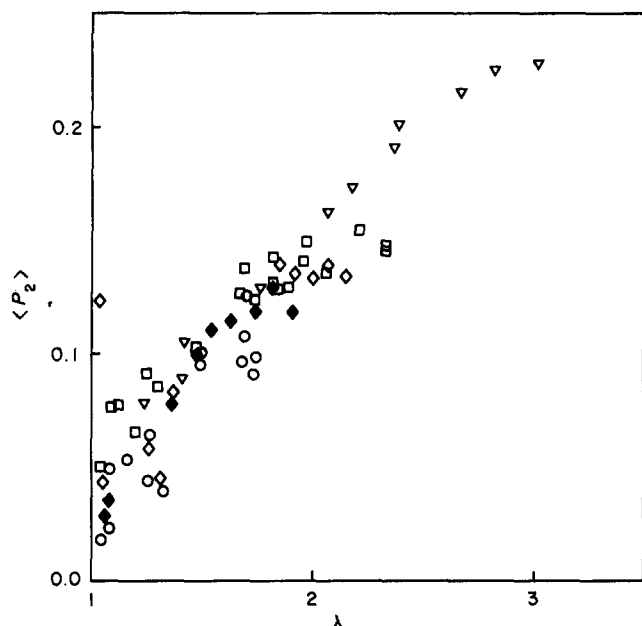


Figure 6  $\langle P_2 \rangle$  vs. extension ratio  $\lambda$  for PMMA below  $T_g$ . Data from WAXS<sup>16,21</sup> in plane strain compression geometry: (○) 20°C; (◆) 40°C; (◇) 60°C; (□) 80°C; (▽) 100°C

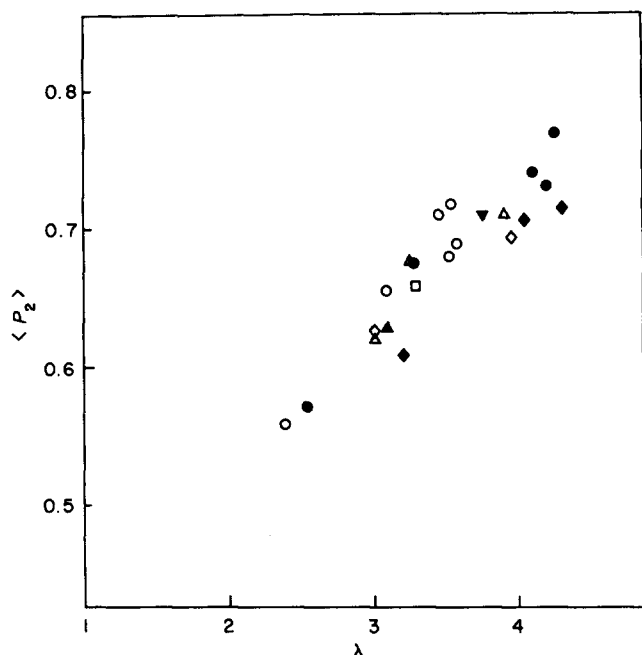


Figure 7  $\langle P_2 \rangle$  vs. extension ratio for PET drawn below  $T_g$  (data from ref. 33). Note that the vertical scale does not start at zero. Solid symbols refer to material of number-average molecular weight  $M_n$  of 1400, open symbols to material of  $M_n=22\,500$ . Temperature: (◆, ◇) 60°C; (●, ○) 20°C; (▼, ▽) 0°C; (▲, △) -30°C; (□) -60°C

$\delta$ , with data taken from the same WAXS investigations of PMMA as Figures 2 and 6, demonstrates that  $\langle P_4 \rangle$ , the second term in the orientation distribution function, remains very low at all strains whether above or below the glass transition. Comparison with Figure 5 shows the contradiction which this represents with the prediction of the pseudoaffine model that  $\langle P_2 \rangle$  and  $\langle P_4 \rangle$  should be of comparable magnitude at all but the lowest strains.

### APPLYING THE AFFINE MODEL TO NON-CHEMICALLY CROSSLINKED MATERIALS

The network chain in conventional rubber elasticity can be simply taken as the macromolecular chain segment between chemical crosslinks. With this view, and the assumption that network chains interact only via their crosslinks, the familiar trend (characteristic of natural rubber) of a gradually accelerating curve of birefringence against strain may successfully be modelled along with the associated stress-strain behaviour. This success is achieved even without the introduction of a distribution of chain lengths such as would exist in practicable systems.

The same approach can be applied to materials which have few or no permanent chemical crosslinks, but in which molecules are linked by mechanical entanglements. Such entanglements may be genuine topological linkages—for example interlocking closed loops—or more loosely-defined tangles where neighbouring chain segments interact sterically to impede relative motion. The latter will be transient, since the chains will be able to

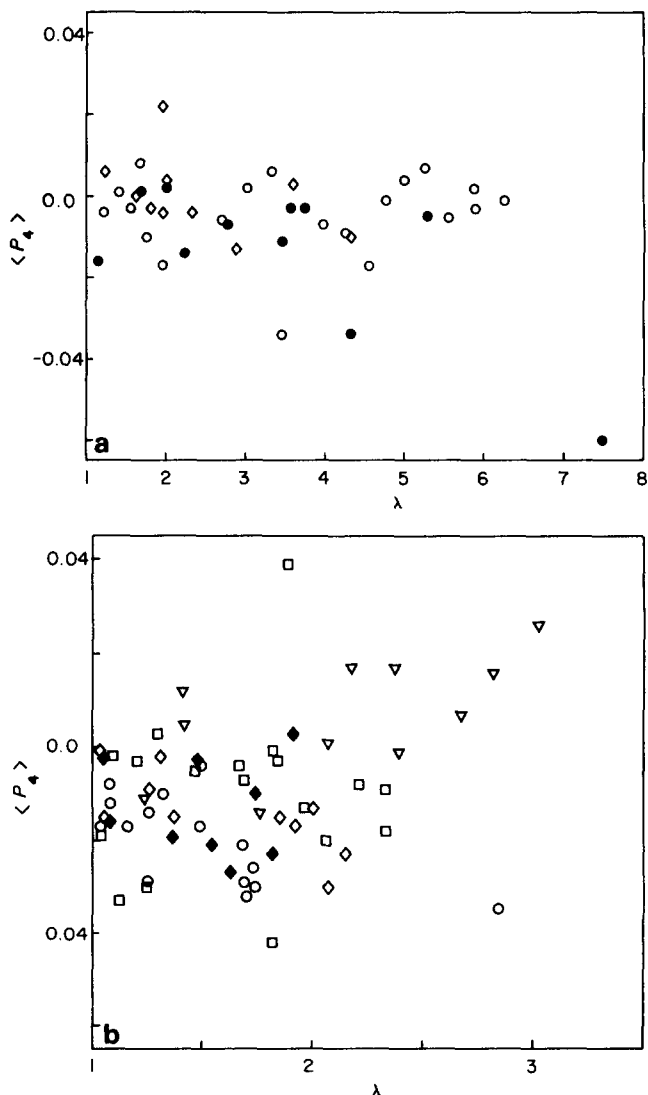


Figure 8 Orientation parameter  $\langle P_4 \rangle$  vs. extension ratio  $\lambda$  for PMMA. Data from WAXS. (a) Above  $T_g$ : (○) plane strain compression, 125°C<sup>16,21</sup>; (●) plane strain compression, 150°C<sup>16,21</sup>; (◇) uniaxial tension, 150°C<sup>22</sup>. (b) Below  $T_g$  (all data refer to plane strain compression): (○) 20°C; (◆) 40°C; (◇) 60°C; (□) 80°C; (▽) 100°C

disentangle themselves by reptation on a suitable time-scale; the former will be permanent, but will differ from chemical crosslinks in that the linkage cannot be associated with a fixed point on the chain. Many systems will involve all these types of linkage, both chemical and mechanical. The significance of the mechanical links is not just that they add to the overall effective crosslink density, but that their contribution may be variable with stress, strain, strain rate, or temperature. The simpler picture of straightforward rubber elasticity may be seen as the limiting case in which chemical crosslinks are sufficiently numerous and effective to swamp any contributions of a mechanical nature.

This rather broader view of an entangled and perhaps crosslinked network model enables one to take a second look at the available orientation-strain data and at the possibility of relating glassy to rubbery behaviour. In the basic affine model, the relationships between the  $\langle P_{2n} \rangle$  parameters and strain are dependent on only one parameter, the number ( $n$ ) of 'statistical random lines' per chain. A particularly useful way of examining experimental  $\langle P_2 \rangle$  data is to take each data point and determine by an iterative method the  $n$  which an affine random chain model would require in order to predict a  $\langle P_2 \rangle$  matching the experimental result. The  $n$  values so obtained can then be plotted against extension ratio  $\lambda$ : Figures 9-12 show this procedure applied to the  $\langle P_2 \rangle$ -strain data discussed above. The standard expressions for  $\langle P_2 \rangle$  as a function of strain are confined to strains below an extension ratio of  $n^{1/2}$ , the limit of the affine model. If however one assumes that a chain, once fully extended, continues to rotate without further change in length, then it is possible to cope with data points which appear to lie beyond the  $n^{1/2}$  limit. This approach involves assumptions which are strictly incompatible, but its proponents<sup>36</sup> argue that it affords a convenient mathematical device for dealing with high-strain data: we, in the same spirit, employ it for the purposes of Figures 9-12.

Several features of the  $n$  vs.  $\lambda$  plots are apparent. Firstly, there is a clear tendency for  $n$  to increase with strain, in an approximately linear fashion. The slope is particularly marked for rubbery thermoplastics, but is evident even in

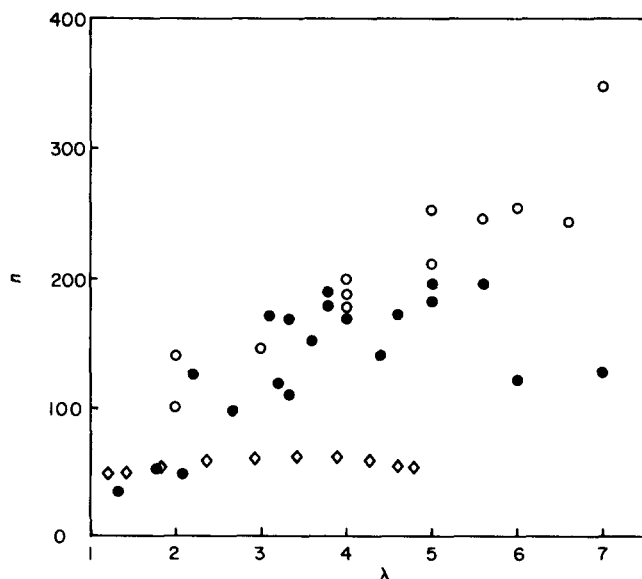


Figure 9 Number of links  $n$  required by an affine model<sup>36</sup> in order to predict a  $\langle P_2 \rangle$  matching the experimental value. Data for *cis*-polyisoprene (natural rubber), as in Figure 1

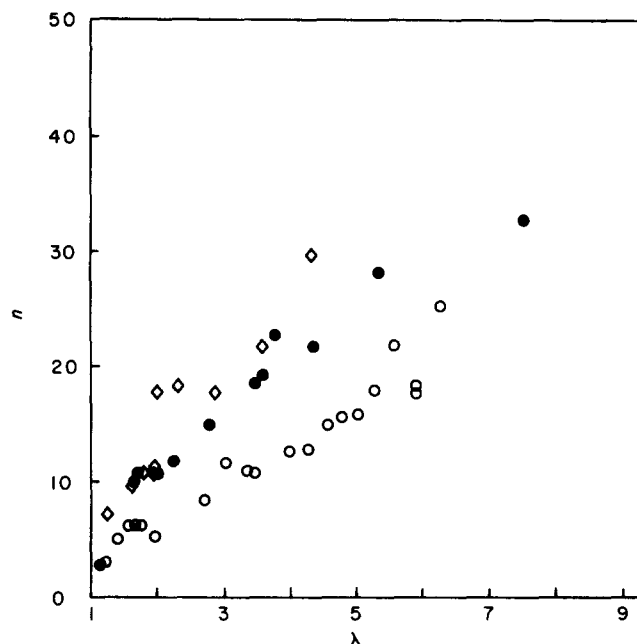


Figure 10  $n$  vs. extension ratio  $\lambda$  for PMMA: WAXS data as in Figure 2: (○) plane strain compression, 125°C; (●) plane strain compression, 150°C; (◇) uniaxial tension, 150°C

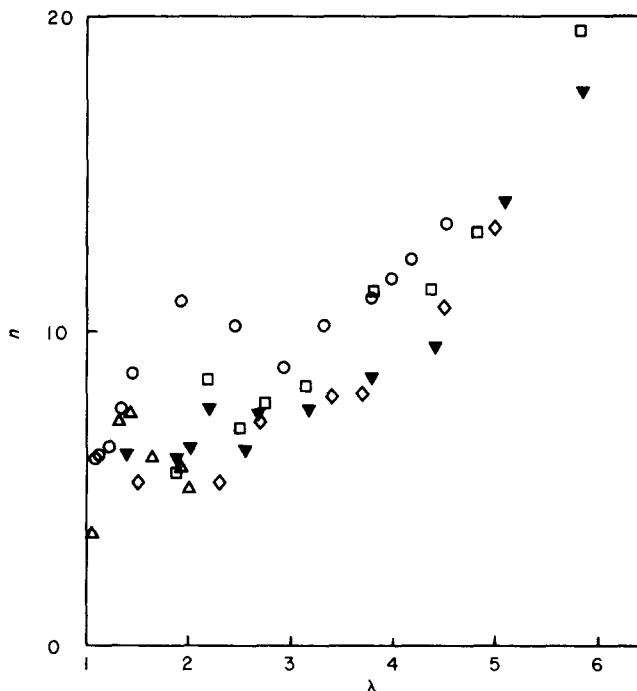


Figure 11  $n$  vs. extension ratio for PET: data as in Figure 3

*cis*-polyisoprene, natural rubber. The downward deviation from linearity in some of the plots for natural rubber – notably the trend in the birefringence-based data of Treloar<sup>8</sup> – may be accounted for by the onset of strain-induced crystallization<sup>20</sup>: if this is so, the tendency is still more solidly based.

Secondly, and again especially in the thermoplastics,  $n$  approaches so low a value at small strains that the admissibility of the statistical basis of conventional rubber elasticity theory becomes questionable, while the ratio of  $n$  at high strains to the zero-strain intercept becomes extremely large.

Taken together, these observations demonstrate that if the affine model is to describe the relationship between

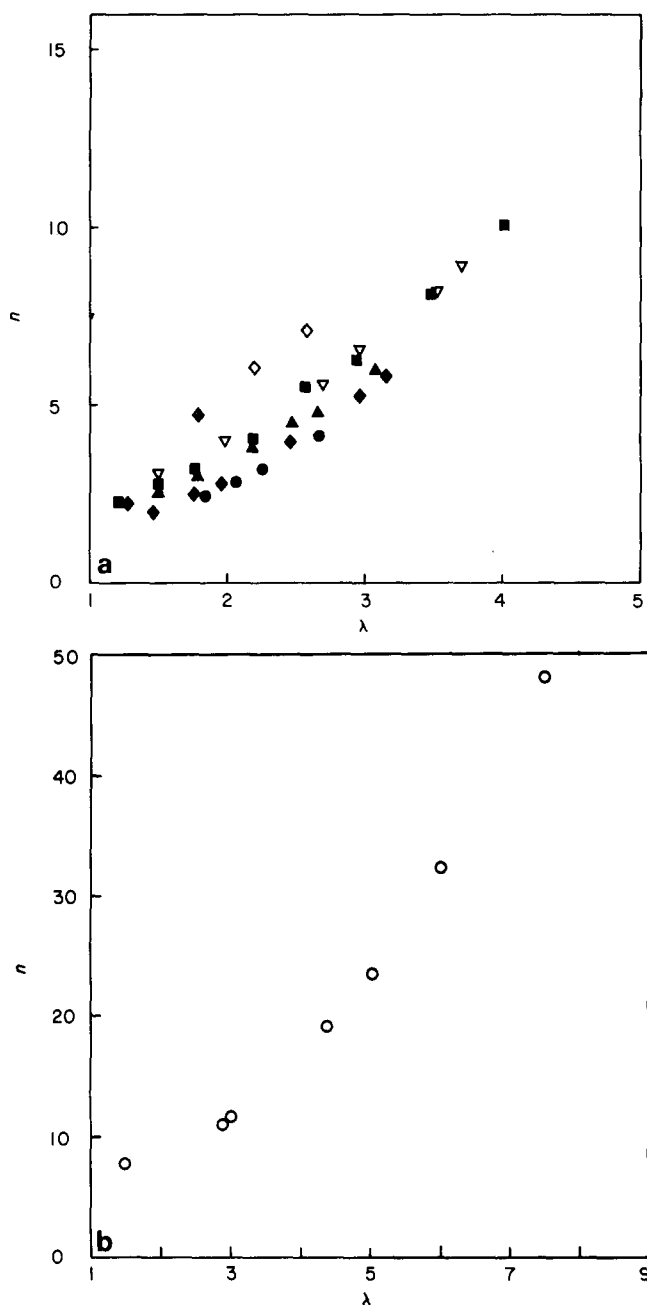


Figure 12  $n$  vs. extension ratio for PVC: data as in Figure 4. Note the different scales in (b)

absolute orientation and strain, very considerable changes in the nature of the supposed random chain will be necessary—both in thermoplastics and to a lesser but significant extent in chemically crosslinked rubbers.

## INTERPRETATION

It is clear from the evidence above that the application of a random chain model to thermoplastics demands some departure from the conventional picture of a statistical chain with a fixed number of equivalent random links. Some of the attractive simplicity of rubber elasticity theory will be lost, but this is perhaps an inevitable consequence of endeavouring to embrace not only a wide range of materials, but also the differing regimes of rubbery and glassy behaviour, within one conceptual framework.

Three basic approaches to the problem can be identified, representing successively more radical departures from the conventional picture of an affinely deforming random chain with fixed  $n$ . The purpose of the present discussion is not to establish a 'correct' one to the exclusion of others, for each has its value; but to outline how they enable orientation-strain data to be interpreted, and to identify some implications for the nature of the polymer chain and the interactions, both intermolecular and intramolecular, which affect its behaviour.

The first approach is to allow the 'equivalent random link' to change—that is, to suppose that under appropriate circumstances the real macromolecular chain becomes less flexible, so that the freely-jointed random chain to which its behaviour may be compared is one with rather fewer and bigger links than before. This view is plausible enough when considering temperature-induced changes. It has long been used to describe, for example, the temperature dependence of birefringence in polyethylene<sup>37</sup>: the chains appear to stiffen with decreasing temperature. At constant temperature, however, the approach is less satisfactory—it is difficult to see how the effective random link could decrease in size as strain increases, particularly if the changes required are to be as drastic as Figures 10 and 11 demand. Indeed, one might have anticipated that the size of the equivalent random link would increase (i.e. the chains stiffen) at high strains, as portions of the molecules become fully extended.

Though this approach would allow any  $\langle P_2 \rangle$ -strain plot to be fitted by an affine model (if one takes it far enough even an apparently pseudoaffine relationship could be described by very rapid changes with strain of the number of random links per network segment), there is little evidence that variations on a sufficiently extensive scale are occurring. It is true that limited conformational changes may accompany deformation (e.g. in PET<sup>24,38</sup>), but to account for apparent variations in  $n$  between, say, 1–5 at low strains and 30–50 at high strains one would have to appeal to changes in chain stiffness as drastic as those associated with major transitions such as  $T_g$ . In PMMA, perhaps the best-characterized non-crystalline polymer from a structural viewpoint, significant conformational changes may be ruled out<sup>39</sup>.

The second approach is to suppose that the network points themselves are labile—so that the equivalent random link can remain of fixed size, while the number of them per chain segment (between effective crosslinks) varies. This would of course affect the number of chain segments per unit volume,  $N$ , and in terms of rubber elasticity theory an increasing  $n$  from this source would imply a proportionate decrease in  $N$  and thus in the rubber modulus  $NkT$ . Nonetheless, the considerations above regarding mechanical entanglements (which will act as crosslinks) suggest that part, at least, of the mechanical contribution to the overall apparent crosslink density will be metastable. Even those mechanical tangles which for topological reasons cannot disappear entirely will nevertheless be able to move along the chain to some degree, along the lines of the slip-link representation of a confined polymer chain<sup>40</sup>.

Treatments which fall within the scope of this second general approach have been set out by several authors. Raha and Bowden<sup>41</sup>, in their studies of optical anisotropy in glassy PMMA, suggest that the density of 'cohesion points' (effective crosslinks) is a function both of tempera-

ture and of strain. They support this interpretation by pointing out that in PMMA 'cohesion points' may correspond to secondary valence bonds, which will clearly be less stable than true chemical crosslinks. The authors suggest however that after yield the polymer behaves with 'rubber-like freedom'; they do not consider in detail how rubber-like deformation itself may be influenced by variations in apparent crosslink density.

Raha and Bowden's concept of essentially electrostatic 'cohesion points' is followed in part by Kahar and others<sup>42</sup> in a later study of the stress-optical properties of PMMA. The latter authors supplement these cohesion points, however, by a 'permanent' (their quotation marks) network of entanglements which remains stable above  $T_g$ . They proceed to a phenomenological description of deformation and shrinkage behaviour, along the lines of the Mooney-Rivlin equation, and avoid proposing a specific molecular mechanism. More recently, Smith<sup>43</sup> has developed a phenomenological model for the analysis of both birefringence and thermal expansivity data for deformed glassy polymers: his suggestion is that the entanglement network is stable up to extension ratios of 5 to 6, and that entanglement slippage occurs at higher strains with the (perhaps unlikely) implication that further deformation destroys virtually all the entanglements.

The third and perhaps most far-reaching approach arises from the realization that orientation is more than just a simple function of strain: chain alignment is for example more rapidly removed during annealing and relaxation than is overall deformation<sup>34,42</sup>. To describe such differences adequately, orientation and strain must be 'decoupled', at least in part.

One of the difficulties of conventional rubber elasticity is the inevitable fact that as deformation proceeds, some chains will begin to reach the maximum extension possible without backbone distortion. They will clearly no longer be able to behave affinely, irrespective of the conformations of their neighbours or of the macroscopic strain level. The various non-Gaussian versions of elasticity theory arrive at the  $n^{1/2}$  limit for affine deformation by making, implicitly, the rather sweeping assumption that all chains reach this stage simultaneously. However, in a real network there will in fact be some chain segments which will be highly extended at the outset (there is a distribution of end-to-end lengths), and some which are short. The presence of these segments will bring about increasing deviations from affine behaviour, beginning at a very early stage in the straining process.

The inevitable existence of very short chain segments led Dobson and Gordon<sup>44</sup> to consider separating the orientational and extensional entropy contributions of network chains. They regard very short chains (as short as 1-2 backbone bonds) as orientationally but not extensionally active—i.e. their end-to-end vectors are capable of changing direction but cannot significantly change in length. A treatment taking into account the entropy contribution of these very short segments led to a stress-strain equation incorporating an additional term in comparison to the classical theory, and this additional term could be identified with the  $C_2$  term of the well-known (but originally empirical) Mooney-Rivlin equation, at least at strains below about 100% (extension ratio  $\lambda = 2$ ). The authors point out that the mathematics in their derivation was in fact performed in early work by Kuhn and Gr $\ddot{u}$  n themselves, but was neglected in the develop-

ment and refinement of rubber elasticity theory by later authors.

Dobson and Gordon's 'orientationally active' chains were considered as short segments between chemical crosslinks, but a more general view is possible in which mechanical entanglements may also lead to portions of molecular chains having only limited scope for changes in length as distinct from direction. Any attempt to describe in detail the effect of these mechanically 'hindered' segments, together with the spectrum of behaviour between the 'short-chain' and 'affine' extremes, would be extremely complex. Nevertheless, useful progress can be made with a very simple approach to the molecular networks as a whole. Brown and Windle have introduced<sup>34</sup> the concept of an 'average constraint' on the extensional part of the deformation process. As in Dobson and Gordon's work, the separation of orientational and extensional contributions to strain is taken as a foundation, but it is seen as applying to all the chains. On this basis a first-order model for rubberlike deformation can be set out, and such a model exhibits the appropriate characteristics of both stress-strain and orientation-strain behaviour. Differences in the orientational response among mechanically and/or chemically crosslinked systems reflect the differing anisotropy of the orienting unit (typically some few repeat units in length) in each case. The introduction of a rate dependence, affecting the longer-range extensional component more strongly than the orientational component, leads to trends paralleling those observed on moving from true rubberlike deformation towards  $T_g$  and the glassy regime. As an example, Figure 13 illustrates the orientation-strain behaviour predicted by the Brown and Windle model in comparison to PET data discussed above.

## DISCUSSION

We have considered a variety of possible models to account for the discrepancies between the classical view of rubber elasticity and the quantitative orientation-strain

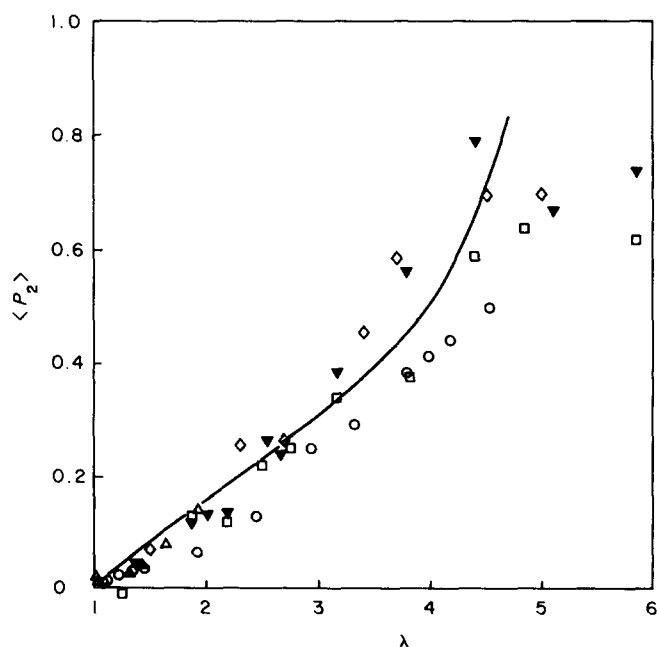


Figure 13  $\langle P_2 \rangle$  vs. extension ratio for PET drawn at 80°C (as Figure 2), compared with the best-fit prediction of a two-component deformation model<sup>34</sup>

behaviour of both crosslinked and uncrosslinked systems. It is perhaps salutary to see the number of seemingly reasonable interpretations that may be placed upon the data. However, we must first consider the implications of the modifications that have been introduced into the basic affine type of model. The affine model is founded upon equilibrium thermodynamics: while such a model may provide a starting point for consideration of orientation in uncrosslinked systems and glasses, one must also be prepared to take account of the influence of non-equilibrium conditions on deformation in these cases. The description of these aspects in terms of entanglements is an attractive proposition in many ways. However, such an approach requires a particular variation with strain in the network structure, while the configurations of the chains between crosslinks change in a genuinely affine manner. So, though perhaps useful as a first order approximation, this approach would appear to flout the precepts of the affine formulation.

If we place some reliance upon the numerical values obtained for  $n$ , the number of statistical segments between effective crosslink points, then at moderate strains (say, of order 100%, i.e.  $\lambda=2$ ) the chain lengths between such points are broadly comparable to estimates of entanglement spacings derived from dynamic compliance measurements (e.g. ref. 46), while extrapolation of Figures 9–12 to zero strain implies rather shorter chain lengths than these estimates would suggest. In making this comparison it must be remembered that the size of a statistical random link would be close to one monomer unit in a flexible molecule such as natural rubber<sup>4</sup>, and rather larger in a stiffer chain such as that of PMMA.

The deformation of glasses might be thought to be dominated by interchain segmental interactions. In a rubber the level of such interchain interactions will naturally be less, but it would be reasonable to assume that the magnitude of the effects would be related to the aspect ratio or anisotropy of the chain segments. In this case we would expect greater perturbation of the affine model in the case of PMMA or PET (aspect ratio of 2) than for the highly flexible chain of natural rubber. This trend is reflected in the steepness of the  $n$  versus strain curves for PMMA or PET compared with natural rubber. In order to confirm these qualitative interpretations we require both additional data and a more firmly based approach with which to handle entanglements (for example reference 40).

An examination of deformation in a crosslinked system would obviously be facilitated by well characterized networks. The use of neutron scattering to monitor the movement of crosslink points would increase the number of different types of data available to fit the opposing models. However, this type of experimentation is clearly not possible in the thermoplastic polymers considered above, and therefore a wider range of studies needs to be considered, including the use of annealing and relaxation measurement.

The studies detailed above indicate the utility of considering molecular orientation as an important component of any attempt to understand the deformation of polymeric systems, whether they be glassy or rubberlike. Such orientation studies need to be quantitative in origin, and to indicate, as wide-angle X-ray scattering measurements do, the nature of the orienting unit. However, these measurements will be to no avail unless existing and

future deformation models predict orientation-strain relationships in addition to the familiar force-extension curves.

## ACKNOWLEDGEMENTS

The financial support of the SERC is gratefully acknowledged.

## REFERENCES

- 1 Kuhn, W. *Kolloid Z.* 1934, **68**, 2
- 2 Kuhn, W. *Kolloid Z.* 1936, **76**, 258
- 3 Kuhn, W. and Gr $\ddot{u}$ n, H. *Kolloid Z.* 1942, **101**, 248
- 4 Treloar, L. R. G. 'The Physics of Rubber Elasticity' (3rd Edn.), Oxford Univ. Press, London, 1975
- 5 James, H. M. and Guth, E. J. *Chem. Phys.* 1947, **15**, 651
- 6 Flory, P. J. *Proc. Roy. Soc. London, Series A* 1976, **351**, 351
- 7 Treloar, L. R. G. *Trans. Faraday Soc.* 1947, **43**, 277
- 8 Treloar, L. R. G. *Trans. Faraday Soc.* 1947, **43**, 284
- 9 Saunders, D. W. *Trans. Faraday Soc.* 1956, **52**, 1414
- 10 Saunders, D. W. *Trans. Faraday Soc.* 1957, **53**, 860
- 11 Saunders, D. W. *Nature* 1950, **165**, 360
- 12 Saunders, D. W. *Trans. Faraday Soc.* 1956, **52**, 1425
- 13 Wilkes, G. L. *J. Macromol. Sci., Rev. Macromol. Chem.* 1974, **10**, 149
- 14 Ward, I. M. (Ed.) 'Structure and Properties of Oriented Polymers', Appl. Sci. Pub., London, 1975
- 15 May, M. J. *Polym. Sci., Polym. Symp. Edn.* 1977, **58**, 23
- 16 Pick, M., Lovell, R. and Windle, A. H. *Polymer* 1980, **21**, 1071
- 17 Windle, A. H. in 'Developments in Oriented Polymers' (Ed. I. M. Ward), Applied Science Pub., London, 1982
- 18 Mitchell, G. R. and Windle, A. H. *Polymer* 1983, **24**, 285
- 19 Mitchell, G. R. and Windle, A. H. *Colloid Polym. Sci.* 1982, **260**, 754
- 20 Mitchell, G. R. *Polymer* 1984, **25**, 1562
- 21 Mitchell, G. R., Pick, M. and Windle, A. H. *Polymer* 1983, **24** (Commun.), 16
- 22 Brown, D. J. and Mitchell, G. R. *J. Polym. Sci., Polym. Lett. Edn.* 1983, **21**, 341
- 23 Rietsch, F., Duckett, R. A. and Ward, I. M. *Polymer* 1979, **20**, 1133
- 24 Cunningham, A., Ward, I. M., Willis, H. A. and Zichy, V. *Polymer* 1974, **15**, 749
- 25 Nobbs, J. H., Bower, D. I., Ward, I. M. and Patterson, D. *Polymer* 1974, **15**, 287
- 26 Nobbs, J. H., Bower, D. I. and Ward, I. M. *Polymer* 1976, **17**, 25
- 27 Purvis, J. and Bower, D. I. *J. Polym. Sci., Polym. Phys. Edn.* 1976, **14**, 1461
- 28 Hibi, S., Maeda, M., Kubota, H. and Miura, T. *Polymer* 1977, **18**, 137 and 143
- 29 Rider, J. G. and Hargreaves, E. J. *Phys. D.* 1970, **3**, 993
- 30 Kashiwagi, M. and Ward, I. M. *Polymer* 1972, **13**, 145
- 31 Kratky, O. *Kolloid Z.* 1933, **64**, 213
- 32 Ward, I. M. 'Mechanical Properties of Solid Polymers', Wiley, N.Y., 1971
- 33 Foot, J. S. and Ward, I. M. *J. Mater. Sci.* 1975, **10**, 955
- 34 Brown, D. J. and Windle, A. H. *J. Mater. Sci.* 1984, **19**, 1997, 2013 and 2039
- 35 Donald, A. M. and Kramer, E. J. *J. Polym. Sci., Polym. Phys. Edn.* 1982, **20**, 899
- 36 Nobbs, J. H. and Bower, D. I. *Polymer* 1978, **19**, 1100
- 37 Volungis, R. J. and Stein, R. S. *J. Chem. Phys.* 1955, **23**, 1179
- 38 Cavanaugh, D. B. and Wang, C. H. *J. Polym. Sci., Polym. Phys. Edn.* 1981, **19**, 1273
- 39 Lovell, R. and Windle, A. H. *Polymer* 1979, **20**, 175
- 40 Ball, R. C., Doi, M., Edwards, S. F. and Warner, M. *Polymer* 1981, **22**, 1010
- 41 Raha, S. and Bowden, P. B. *Polymer* 1972, **13**, 174
- 42 Kahar, S., Duckett, R. A. and Ward, I. M. *Polymer* 1978, **19**, 136
- 43 Smith, K. J. *Polym. Eng. Sci.* 1984, **24**, 205
- 44 Dobson, G. R. and Gordon, M. *Trans. Inst. Rubber Ind.* 1964, **40**, T262
- 45 Ferry, J. D. 'Viscoelastic Properties of Polymers' (3rd Edn.), Wiley, New York, 1980, Ch. 13B